*Ceramics International* **21** (1995) 77–83

# Investigation of Silicon Nitride Composites Toughened with Prenitrided $TiB_2$

**Jow-Lay Huang & Shih-Yih Chen**

Department of Materials Science and Engineering, National Cheng Kung University, Tianan, Taiwan

(Received 20 May 1994; accepted 8 June 1994)

**Abstract:** Titanium diboride, which was prenitrided in various conditions, was incorporated into $Si_3N_4$ before hot pressing. The TiN coating substantially reduced the chemical reaction between $TiB_2$ and the $Si_3N_4$ matrix. The thickness of TiN coating played an important role in the chemical stability of $TiB_2$ in the $Si_3N_4$ matrix and the strain compatibility at interfaces. The fracture toughness of $Si_3N_4$ was enhanced 33% with prenitrided-$TiB_2$ particles (20% by volume). Crack deflection was the major toughening mechanism, but the microcracking mechanism could also play a role.

## 1 INTRODUCTION

The area of ceramic-reinforced $Si_3N_4$ has drawn considerable attention over the past decades because of its substantial improvements in the mechanical, chemical and thermal properties and reliability.

Titanium diboride exhibits a relatively high melting point, large Young's modulus, hardness, thermal expansion coefficient and thermal conductivity among ceramics. It is therefore currently being developed as an armour material and applied towards toughening a ceramic matrix. A toughness enhancement of 45–90% through incorporation of $TiB_2$ into SiC was reported by Janney[1] and McMurtry[2]. The toughness of $Al_2O_3$ also improved 70% by incorporation of $TiB_2$, as reported by Liu.[3]

Only a few reports on the $TiB_2/Si_3N_4$ system are published.[4–6] Although a possible reaction between $TiB_2$ and $Si_3N_4$ was reported,[6] it remains unclear how $TiB_2$ affects the microstructure and mechanical properties; this topic was one objective of this work.

Huang and Chen[7] reported that titanium nitride has a good chemical stability in $Si_3N_4$ up to a temperature greater than 1800°C. Another major objective of this study was to explore the feasibility of inhibiting chemical interactions between $TiB_2$ and $Si_3N_4$ by means of coating TiN onto $TiB_2$ particles before hot pressing.

The $TiB_2$ particles were nitrided in $N_2$ at different temperatures and for various durations. The nitridation behavior and morphology of reactants were scrutinized in this investigation. Both pristine and pre-nitrided $TiB_2$ particles up to 20 volume % were incorporated into $Si_3N_4$. Possible interfacial reactions between the dispersed particle and $Si_3N_4$ were examined. The microstructure, developed phases, physical and mechanical properties of the $TiB_2$-containing $Si_3N_4$ composites were explored.

## 2 EXPERIMENTAL PROCEDURE

### *2.1 Nitridation of $TiB_2$ particles*

$TiB_2$ particles were placed in a crucible and nitrided in an alumina-tube furnace in flowing nitrogen gas. The gas was purified by passing through a U-tube containing $P_2O_5$ and silicon gel to remove moisture. The amounts of gas before and after passing samples were monitored by two separate mass flow-meters that were interfaced with a microcomputer. The computer acquired, stored and analyzed the rate of gas consumption and corresponding temperature.

$TiB_2$ particles were nitrided at a ramp rate of 10°C/min up to 1400°C for 1 and 12 h, respec-

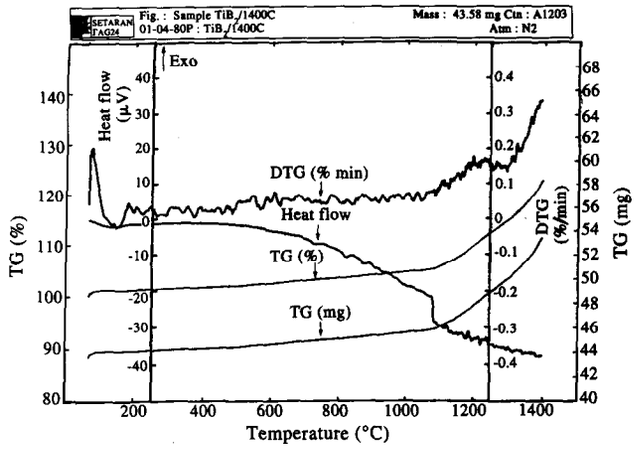


**Fig. 1.** DTA/TGA analysis of $TiB_2$ nitriding from 70°C to 1400°C with a heating rate of 10°C/min.

tively. DTA and TGA were used to monitor the thermal flow and the alteration of mass during nitridation.

### 2.2 Powder preparation

Silicon nitride powder (H.C. Starck LC12, size 0·6 μm) was mixed with yttria (Molycorp 5603X, 6 mass%) and alumina (Alcoa A16SG, 2 mass%) in a polyurethane bottle with high-purity silicon nitride balls and ethanol for 22 h. Titanium diboride (H. C. Starck B, 6 μm, 20% by volume), was dispersed with an ultrasonic probe in ethanol, added

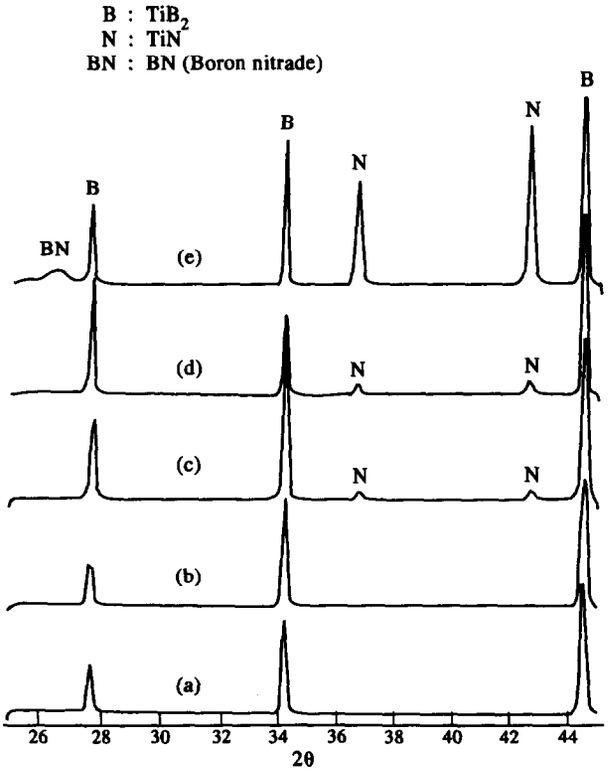


**Fig. 2.** X-ray diffraction profiles of as-received $TiB_2$ and prenitrided $TiB_2$ (a) $TiB_2$ (as received), (b) nitrided $TiB_2$ (1100°C, 1 h), (c) nitrided $TiB_2$ (1200°C, 1 h), (d) nitrided $TiB_2$ (1400°C, 1 h), (e) nitrided $TiB_2$ (1400°C, 12 h).

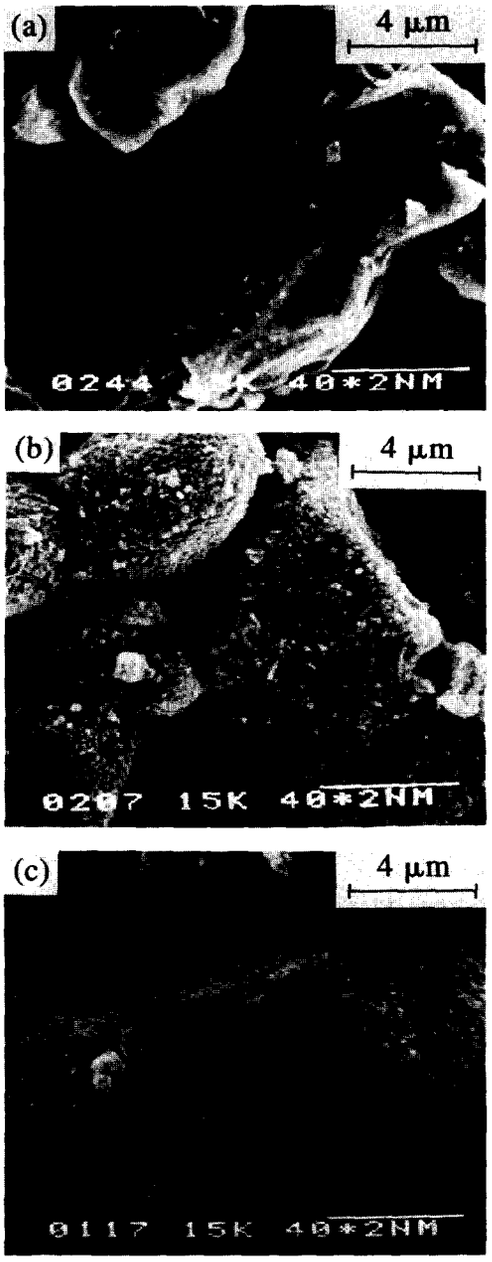


**Fig. 3.** SEM photographs showing the surface morphology of (a) as-received $TiB_2$; (b) $TiB_2$ nitrided at 1400°C for 1 h; (c) $TiB_2$ nitrided at 1400°C for 12 h.

to the $Si_3N_4$ slurry, and milled with PE balls for an additional two hours with a charge to ball ratio of 1:8.

The slurry was then ultrasonically dispersed, dried in a rotating vacuum condenser, baked until dry, ground with mortar and pestle, and screened through a 100-mesh screen.

**Table 1. Sample codes and corresponding compositions**

| Sample code | Composition |
|---|---|
| SN | $Si_3N_4$+$Y_2O_3$(6%)+$Al_2O_3$(2%) |
| 2TB | SN+20 vol% $TiB_2$ |
| 2NTB1 | SN+20 vol% prenitrided $TiB_2$ (nitrided at 1400°C, 1 h) |
| 2NTB12 | SN+20 vol% prenitrided $TiB_2$ (nitrided at 1400°C, 12 h) |

### 2.3 Hot pressing

Samples were hot-pressed at 1750°C under nitrogen in a graphite furnace (Fuji Dempa High Multi 5000) for 1 h at a pressure of 24·5 MPa. Sample codes and the corresponding compositions are illustrated in Table 1.

### 2.4 Flexural strength

Testing samples were machined into bars with dimensions 3×4×50 mm and polished to 15 $\mu$m before conducting a four-point bending test on a universal testing machine (Shimadzu AGS-500D) at a loading rate of 0·5mm/min. Sample edges were chamfered before testing for the purpose of minimizing variation due to stress concentration. The inner and outer spans used for testing were 20 mm and 40 mm, respectively (ASTM E855-81).

### 2.5 Fracture toughness

Fracture toughness was measured according to the surface indentation technique following Evans' derivation.[12] Samples were finely polished to 1 $\mu$m before applying a microhardness indent at 50 kg for 15 s.

## 3 RESULTS AND DISCUSSION

### 3.1 Nitridation of $TiB_2$

Nitridation of $TiB_2$ particles was analyzed by DTA/TGA from 70°C to 1400°C with a heating rate of 10°C/min, and results are shown in Fig. 1. The mass gained during nitridation initially increased slowly, then rapidly and continuously up to 1400°C. Results of heat flow revealed an abrupt absorption of heat at temperatures above 1100°C.

In order to further investigate the nitridation behavior of $TiB_2$, the $TiB_2$ particles were continuously heated from 1100°C to 1400°C for 1–12 h and examined by X-ray diffraction (Fig. 2). Results indicated that TiN started forming at temperatures above 1200°C and the proportion of TiN increased as the hot pressing temperature was increased. A trace of BN was detected when the $TiB_2$ was nitrided at 1400°C for 12 h.

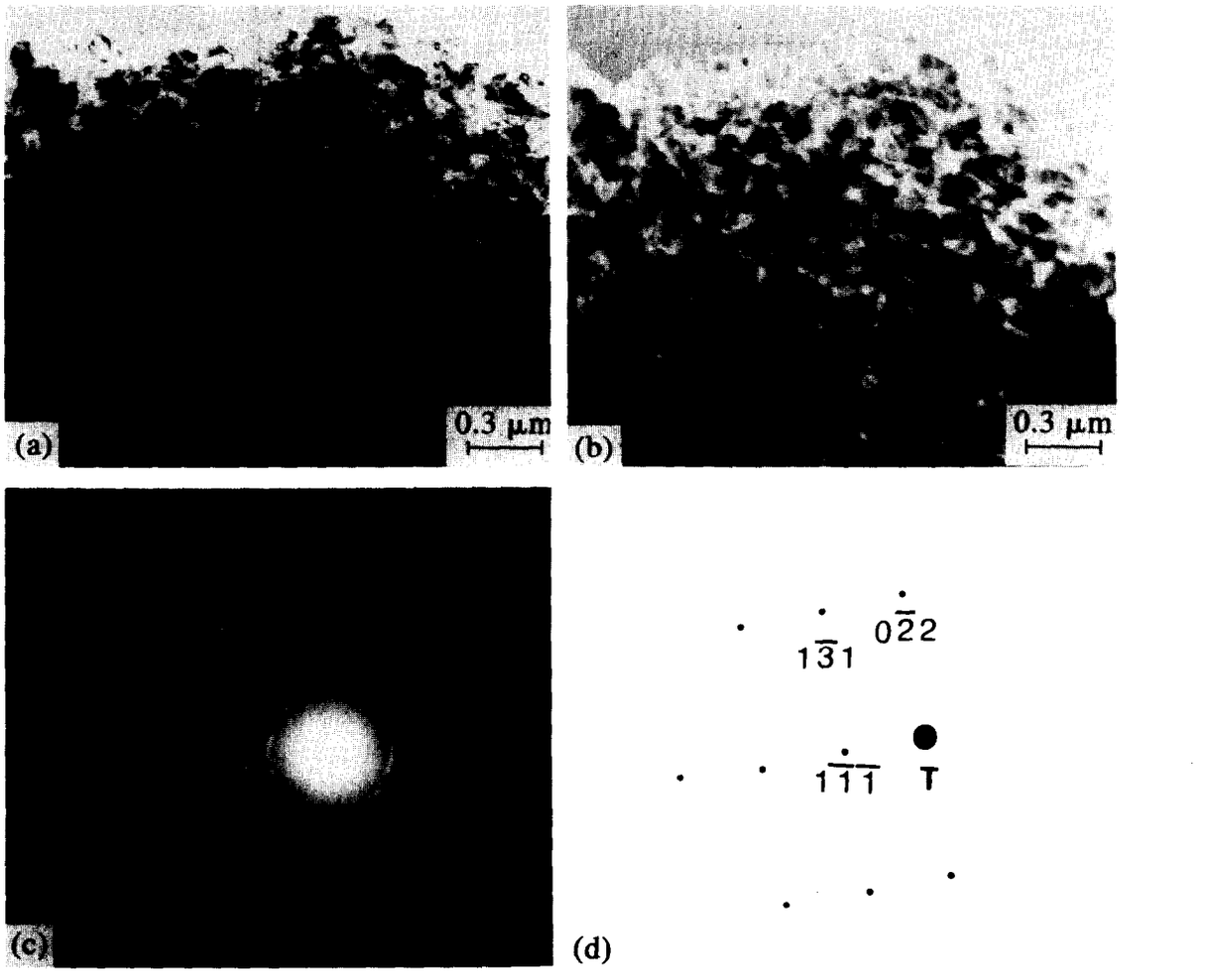


**Fig. 4.** TEM of nitrided $TiB_2$ (1400°C 12 h); (a) bright-field image, (b) dark-field image, (c) electron diffraction pattern of <422> zone axis, (d) analysis of diffraction pattern.

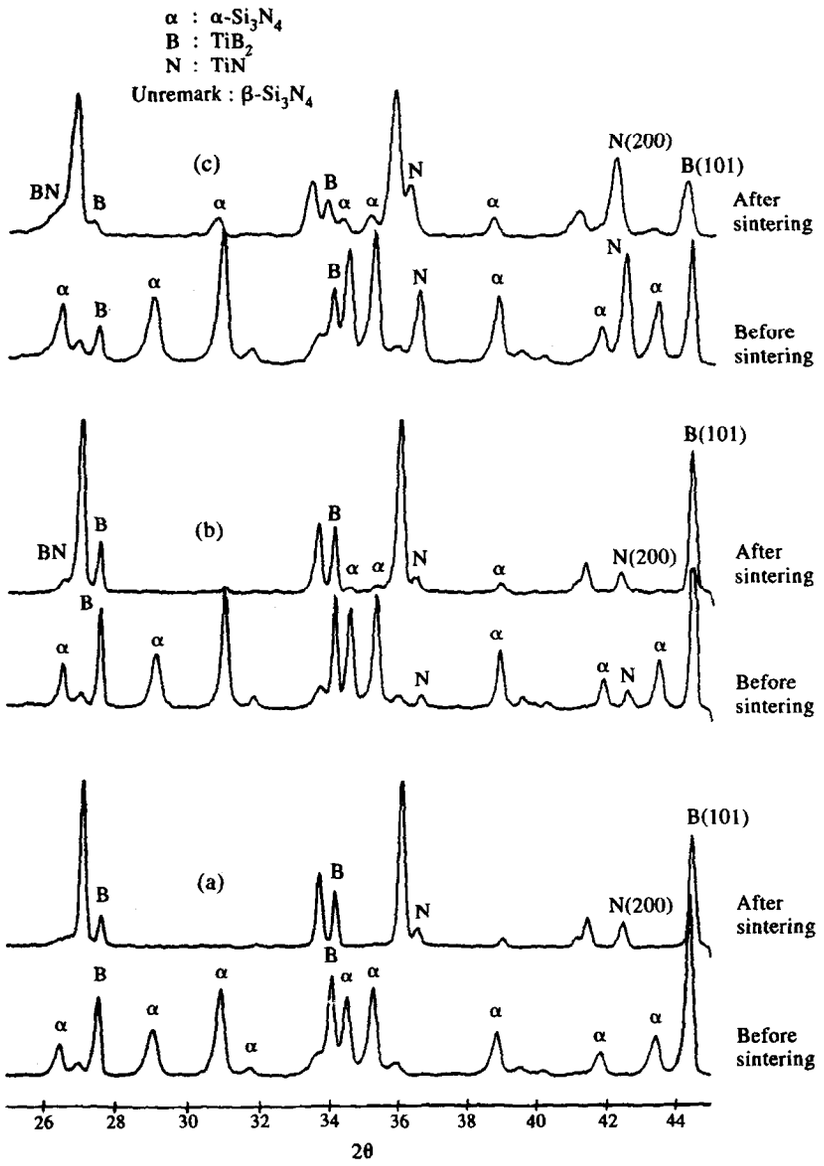


**Fig. 5.** X-ray diffraction profiles of (a) 2TB, (b) 2NTB1 and (c) 2NTB12; results for both before and after hot pressing are shown.

### *3.2 Morphology of nitrided-$TiB_2$ particles*

A typical SEM photomicrograph showing the surface morphology of pristine and nitrided $TiB_2$ particles is presented in Fig. 3. The surfaces of $TiB_2$ particles appeared completely covered with dense and small particles after being nitrided at 1400°C [Fig. 3(b) and (c)]. Further examination and phase identification were conducted using TEM (model JEOL-2000CX) with SAD on the nitrided $TiB_2$ particles. Bright and dark field SAD microscopy photographs of $TiB_2$ nitrided at 1400°C for 12 h are shown in Fig. 4. The small particles adhered on the $TiB_2$ surfaces were identified according to TEM diffraction patterns as FCC TiN [Fig. 4(c) and (d)].

Some nitrided-$TiB_2$ particles were ball milled with PE balls for 2 h and examined under the SEM. The TiN coating still looked intact, which indicated that adhesion between $TiB_2$ and the TiN coating was quite good.

### *3.3 Chemical reactions between $TiB_2$ and the $Si_3N_4$ matrix*

XRD results of 2TB, 2NTB1 and 2NTB12 samples that were hot pressed at 1750°C for 1 h are shown in Fig. 5. The TiN peaks invariably increased after hot pressing, no matter whether the $TiB_2$ was nitrided or not.

The proportions of TiN before and after hot pressing were calculated from the integrated area of the peaks. A 20% TiN increase was detected in the 2TB composite, much larger than the 7–10% in the 2NTB1 and 2NTB12 samples. It was therefore quite obvious that the prenitriding of $TiB_2$ particles effectively diminished the chemical interactions between $TiB_2$ and $Si_3N_4$ during hot pressing.

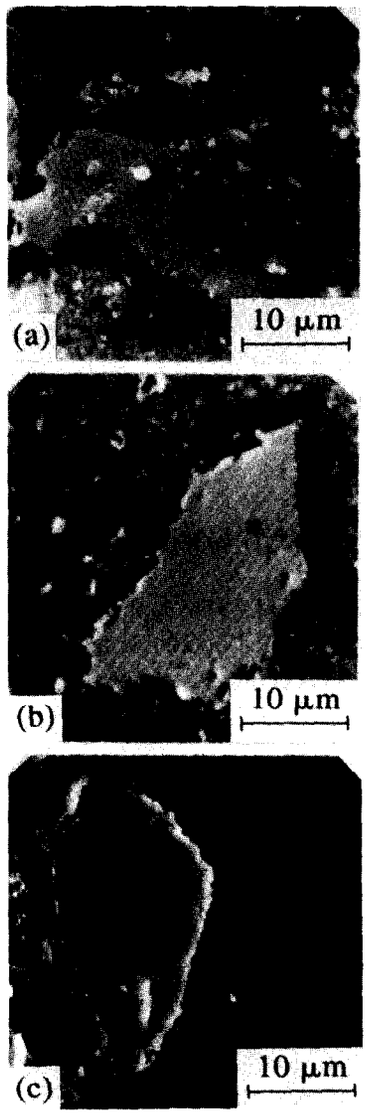


**Fig. 6.** SEM photographs showing microstructure of hot-pressed (a) 2TB, (b) 2NTB1, and (c) 2NTB12.

Some large $TiB_2$ particles were examined under SEM. Numerous pores were found near interfaces in the 2TB samples along a reaction zone[6] [Fig. 6(a)]. Circumferential microcrackings were observed around nitrided-$TiB_2$ particles in hot pressed 2NTB12 samples [Fig. 6(c)]. These microcrackings possibly resulted from a large thermal mismatch between the thick TiN coating and $Si_3N_4$.

However, the hot-pressed 2NTB1 samples appeared to be dense and the interfaces looked quite intact [Fig. 6(b)]. The thin layers around the prenitrided $TiB_2$ particles were identified as TiN.

### *3.4 Effects of prenitrided-$TiB_2$ on the transformation of alpha to beta $Si_3N_4$*

The fraction transformation of alpha-to-beta $Si_3N_4$ in SN, 2TB, 2NTB1 and 2NTB12 samples were calculated from XRD results according to Gazara's derivation[8] (Fig. 7). Approximately 10–20% alpha phase remained in SN, 2NTB1 and 2NTB12 samples after hot pressing at 1750°C. All the alpha phase was converted to beta in 2TB, however, at the same temperature.

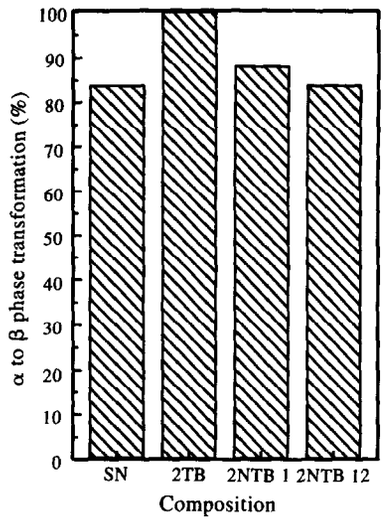


**Fig. 7.** Fraction of phase transformation of $\alpha$-$Si_3N_4$ to $\beta$-$Si_3N_4$ for SN, 2TB, 2NTB1 and 2NTB12; samples were hot-pressed at 1750°C for 1 h.

It was reported that addition of $TiB_2$ enhanced the phase transformation in $Si_3N_4$ due to altered viscosity and composition of boundary phases.[6,7] The conversion of alpha to beta was obviously inhibited as the duration of nitridation of $TiB_2$ particles was increased (Fig. 7). This observation could be more indirect evidence that the TiN coating insulated $TiB_2$ particles from the $Si_3N_4$ matrix and substantially hindered the chemical reaction between $TiB_2$ and $Si_3N_4$ during hot pressing.

### *3.5 Flexural strength*

The four-point bend strength of SN, 2TB, 2NTB1 and 2NTB12 samples are shown in Fig. 8. The strength of $TiB_2$-incorporated $Si_3N_4$ samples was

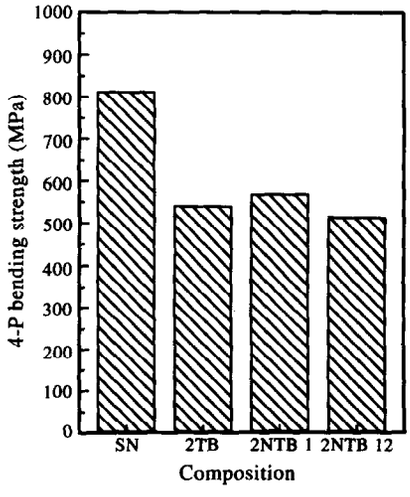


**Fig. 8.** Flexural strength of SN, 2TB, 2NTB1 and 2NTB12; sample were hot-pressed at 1750°C for 1 h in $N_2$ at $10^5$ Pa.

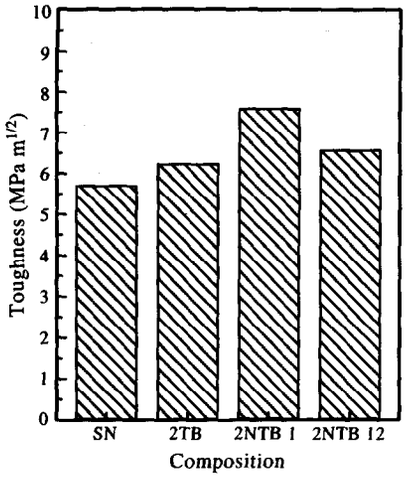


**Fig. 9.** Fracture toughness of SN, 2TB, 2NTB1 and 2NTB12; samples were hot-pressed at 1750°C for 1 h in $N_2$ at $10^5$ Pa.

lower than that of monolithic $Si_3N_4$. This was probably due to the occurrence of microcrackings associated with the incompatibility in CTE and Young's modulus between the $Si_3N_4$ matrix and $TiB_2$.

Further examination of the fractured surfaces indicated that cracks were deflected and then propagated along the interfaces between the $TiB_2$ and $Si_3N_4$ matrix. No obvious transgranular fracture was observed.

### 3.6 Fracture toughness

Results of fracture toughness for $TiB_2$-incorporated $Si_3N_4$ are shown in Fig. 9. The toughness for 2TB, 2NTB1 and 2NTB12 composites was 10–35 percent greater than that of monolithic $Si_3N_4$.

That localized stress can occur around inclusions, due to distinct thermal expansion and elastic properties between the inclusion and matrix, was previously reported.[9] The $TiB_2$ particles have a greater coefficient of thermal expansion (CTE $Si_3N_4 = 3{\cdot}0 \times 10^{-6}$, CTE $TiB_2 = 8{\cdot}1 \times 10^{-6}$) and elastic modulus ($E_{TiB_2}$ = 544 GPa, $E_{Si_3N_4}$ = 304 GPa) than the $Si_3N_4$ matrix. This effect produced a tangential compressive strain near the particle/matrix interface and diverted the crack around the $TiB_2$ particles.[10] A residual stress of 1914 MPa was calculated by substituting the physical properties of $TiB_2$ and $Si_3N_4$ into Evans' derivation,[10] assuming a fully dense composite.

In order to further examine crack behavior, a microhardness diamond indentor was used to introduce microcrackings on polished surfaces of $TiB_2$-containing $Si_3N_4$ samples. Observations revealed that the crack deflection apparently played an extremely important role in enhanced resistance to crack growth.

An approach of toughening induced by incorporation of second-phase particles subject to microcracking was reported by Evans and Faber; the toughening became appreciable for a narrow distribution of second-phase particles larger than a critical size.[11]

By substituting the physical properties of $TiB_2$ and TiN into Evans' derivation,[11] a minimum critical size of 4·4 $\mu$m was obtained. This size was smaller than the average particle size of $TiB_2$ (6 $\mu$m) used for experiments; the microcracking due to mismatch in strain might have some contribution to the toughening effect. More work is needed to distinguish between the effects of stress and of microcracks.

## 4 SUMMARY AND CONCLUSIONS

(1) Results of DTA/TGA indicated that nitridation of $TiB_2$ particles occurred at a temperature of 1100°C and proceeded continuously with temperature above that.

(2) The formation of TiN increased with increasing temperature. The surfaces of $TiB_2$ particles were fully covered with small FCC TiN particles and a trace of BN was detected after heating at 1400°C.

(3) TiN coating on $TiB_2$ particles substantially diminished the chemical reaction between $TiB_2$ and $Si_3N_4$ at elevated temperatures. The thickness of TiN coating played an important role in the thermal stability of $TiB_2$ in the $Si_3N_4$ matrix and the thermal strain compatibility at interfaces.

(4) The flexural strength of $Si_3N_4$ decreased with the addition of $TiB_2$. This is probably due to the incompatiblity of CTE and Young's modulus between $Si_3N_4$ and $TiB_2$.

(5) The fracture toughness of $Si_3N_4$ was enhanced 35% with the addition of prenitrided $TiB_2$. Crack deflection was the major toughening mechanism but microcracking might also have played some role.

## ACKNOWLEDGEMENT

The authors would like to thank National Science Council of the R.O.C. for its financial support under the contract no. 80-0405-E006-49.

## REFERENCES

1. JANNEY, M. A., *Am. Ceram. Soc. Bull.*, **66**(2) (1987) 325–4.
2. MCMURTRY & GARL H., *Am. Ceram. Soc. Bull.*, **66**(2) (1987) 325–9.
3. LIU, J. & OWNBY, P. D., *J. Am. Ceram. Soc.*, **74**(1) (1991) 241–3.
4. ARTHURS, T. C., MMOSTAGHACI, H. & MURPHY, J. G., *Ceram. Eng. Sci. Proc.*, (1985) 589–607.

5. SHEW, BOR-YUAN & HUANG, J. L., accepted by the *J. Mater. Aci. Eng.* May 18, 1992.
6. KUO, FAN-JIAN & HUANG, J. L., accepted by the *J. Mater. Sci. Eng.*, 1993.
7. HUANG, J. L. & CHEN, S. Y., accepted by the *J. Mater. Res.* 1994.
8. GAZZARA, C. P. & MESSIER, D. R., *Am. Ceram. Soc. Bull.*, **56**(9) (1977) 777.
9. EVANS, A. G., *J. Mater. Sci.*, **9** (1974) 1145.
10. FABER, K. T. & EVANS, A. G., Crack deflection process-I theory. *Acta Metall.*, **31**(4) (1983) 565.
11. EVANS, A. G. & FABER, K. T., *J. Am. Ceram. Soc.*, **64**(7) (1981) 394.
12. EVANS, A. G. & CHARLES, E. A., *J. Am. Ceram. Soc.*, **58**(7,8) (1976) 371–2.